A matter of course

Generating optimal manufacturing instructions from a structural layup plan of a wind turbine blade

Krogh, Christian; Hermansen, Sebastian Malte; Lund, Erik; Kepler, Jørgen Asbøll; Jakobsen, Johnny

Published in:
Composites Part A: Applied Science and Manufacturing

DOI (link to publication from Publisher):
10.1016/j.compositesa.2023.107599

Publication date:
2023

Document Version
Publisher's PDF, also known as Version of record

Composites: Part A 172 (2023) 107599

Contents lists available at ScienceDirect

Composites Part A

journal homepage: www.elsevier.com/locate/compositesa

A matter of course: Generating optimal manufacturing instructions from a structural layup plan of a wind turbine blade

Christian Krogh *, Sebastian M. Hermansen, Erik Lund, Jørgen Kepler, Johnny Jakobsen

Department of Materials and Production, Aalborg University, Fibigerstraede 16, 9220 Aalborg, Denmark

ARTICLE INFO

Dataset link: http://dx.doi.org/10.17632/3mh3ghrz67

Keywords:
Draping
Wind turbine blades
Laminated composites
Glass fiber fabric
Optimization

ABSTRACT

Design and manufacturing are highly interlinked when it comes to laminated composites, e.g. wind turbine blades. The structural design defined through the layup plan is not necessarily straightforward to realize during manufacturing. The sheer size of a typical blade means that multiple courses, or roll-widths, of glass fiber must be placed in the casting mold. Further, the layup plan is typically coarsely defined and uses idealized fiber angles. This paper deals with the specification of the individual fabric courses based on an overall layup plan. The courses are modeled using a kinematic draping algorithm and a genetic algorithm optimization routine determines their placement under the consideration of drapability (producibility), structural performance, material waste and practical placement concerns. The results highlight the isolated impact of the different criteria using smaller models. Afterwards, a full 30-layer stack of UD plies is optimized to a feasible course specification with a favorable criteria balance.

1. Introduction

Wind turbines are a key technology in the transition to more renewable energy and with the increasing rotor diameters (currently 220+ m), ever more energy can be harvested from a single turbine. At the same time, this growth challenges the manufacturing of the blades both practically and economically. As the blades constitute a fair part of the total expenses, they naturally have a noticeable impact on the price of the produced energy. A wind turbine blade is made as a laminated composite structure and the manufacturing cost is particularly driven by the manual placement of large amounts of glass fiber fabric material in the blade mold. To this end, current trends in the wind turbine blade industry concern the exploration of *preforms*, i.e. smaller pre-fabricated stacks of fiber material formed to near-net shape, as well as the use of automation. The latter is not only expected to contribute to the cost savings directly but also offer more control of the placement of the fabric material in the mold as well as reducing the associated heavy, repetitive manual labor.

The layup of the blade, i.e. the specification of the layers and the material types of which they consist, is created by the structural designers. During the design phase, simplified fabric layers are typically used, i.e. covering certain regions/patches of the blade mold and with nominal fiber angles. One example is an overall 0° layer that covers the entire width of the mold surface e.g. from the root until a specified length coordinate. Subsequently, the structural layup must be translated into manufacturing instructions. The glass fiber material is supplied in rolls of certain widths and must therefore be placed in specified *courses* to achieve mold coverage (see e.g. Fig. 1 for an illustration of a course). The manufacturing instructions therefore include detailing the length, width and placement of courses while trying to reduce material waste from trimming operations. Ideally, draping effects should also be considered. That is, when placed in a double-curved mold, the fabric courses will need to accommodate local in-plane shear to adapt to the mold surface. This shear will result in changed fiber angles compared to the expected or nominal fiber angle, which will result in an inferior mechanical performance compared to a laminate with ideal fiber angles. The shear will potentially also result in producibility issues if the required shear exceeds the material limit.

The draping behavior of a fabric can for instance be analyzed with a kinematic draping model [1]. Commercial implementations of such models are for instance available with Composites Modeler for Abaqus/CAE [2], Ansys ACP [3] and Fibersim [4]. The kinematic draping algorithm assumes that the extensional stiffness of the rovings is infinite and the shear stiffness of the fabric is zero. The former is justified from the high modulus of structural fibers whereas the latter is due to the fact that shear is the governing deformation mechanism during draping and that the shear stiffness in general is weak [5]. Under these assumptions, the fabric can be modeled as a grid of pin-jointed cells. The draped configuration on a mold can be predicted with reasonable accuracy (as long as the shear angles are moderate in

* Corresponding author.
E-mail address: ck@mp.aau.dk (C. Krogh).

https://doi.org/10.1016/j.compositesa.2023.107599
Received 16 January 2023; Received in revised form 29 March 2023; Accepted 2 May 2023
Available online 6 May 2023

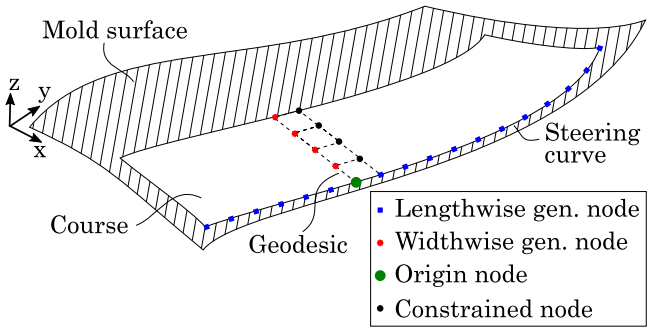

Fig. 1. Draping of fabric course using kinematic draping algorithm.

magnitude) and a low computational effort compared to other draping analysis approaches.

At this point it should be mentioned that also mechanical draping models have been developed, often within the framework of the finite element (FE) method [6,7]. While such models are generally recognized to give more accurate draping predictions – in particular by taking the boundary and process conditions into account – they are also more computationally expensive to evaluate and typically require a series of accurate material data. In this study, only the final draped configuration is of interest, and achieving this configuration is expected to be realistic with the appropriate process equipment. Therefore, the additional modeling complexity is not needed. Notice though, that at a later step in the development, a dedicated process model could become very relevant.

The low computational expense of kinematic draping models favors the use of optimization techniques to determine a desired draping pattern based on some criteria. A number of researchers have studied this combination.

Skordos et al. [8] used a commercial kinematic draping code along with a genetic algorithm (GA) to optimize the draping pattern of a composite helmet. The authors used both single- and multi-objective formulations, i.e. by considering the absolute maximum shear angle and the average shear angle. The design variables included the starting point, starting drape direction and pre-shear. Both kinds of formulations proved successful and also reduced the solution time drastically from that of an exhaustive search. See also the study by Weiland et al. [9].

Cost/weight optimization of a C-spar laminate was conducted by Kaufmann et al. [10]. This work builds upon previous publications by the research group by including a draping modeling module. Here, Composites Modeler for Abaqus/CAE was used for the draping analysis. As the authors note, the reasons to include the draping model were "(a) provide the cost model with more detailed manufacturing knowledge, (b) to perform a structural analysis with fiber angles closer to reality and producibility constraints, and (c) to show that the choice of the draping strategy can influence the cost and weight balance of a component". The objectives considered were fiber angle deviation (difference between actual and nominal fiber orientation of a ply, e.g 0/90°), the magnitude of the computed shear angles, raw material usage and cut length (perimeter of ply shapes). In an effort to save computational time, the authors used the draping model to generate a *draping knowledge base* by sweeping through some combinations of chosen seed points and reference angles. Next, the best plies were used in the gradient-based cost/weight optimization.

Köke et al. [11] presented a method using graph theory and the local Gaussian curvature of the mold to determine the most applicable starting points and directions for draping on arbitrary surface. It is not clear though, how this approach can be combined with more criteria.

Draping optimization of so-called "Continuous-Discontinuous Fiber-Reinforced Composite Structures" was studied by Fengler et al. [12]. The approach was to use a genetic/evolutionary algorithm in combination with a kinematic draping model. A warpage simulation was also included to account for curing effects.

Fiber patch placement was studied by Kussmaul et al. [13] in terms of optimum laminate design. This production technique involves the automatic placement of a large number of small patches of fabric material on a mold. The study involved a kinematic draping model to assist in the placement of the patches.

While the above mentioned studies include useful elements and concepts, none of them consider the fabric material in the form of courses of fixed width. The overarching goal of this paper is to present a method for creating the specifications of each individual course based on an overall design with simplified layers. This specification is based on an optimization routine that takes the drapability (producibility), structural performance, material waste and practical placement concerns into account. The rest of the paper is organized as follows: Section 2 describes the test mold and fabric material system as well as the algorithm behind the kinematic draping model in brief. Section 3 explains the optimization problem formulation including design variables and criteria. Section 4 presents the results of optimized courses in the test mold including studies with variation of parameters and an investigation of the structural performance. Sections 5 and 6 complete the paper with a discussion of the findings and a conclusion.

2. Draping analysis

This study relies on a kinematic draping model of a glass fiber fabric coupled with an optimization routine. First, the analyzed test mold and fabric material are introduced. Next, an outline of the draping model is described, and lastly a post-evaluation of the structural performance is detailed.

2.1. Mold and fabric material system

The material of this study is a glass fiber quasi-unidirectional (UD) non-crimp fabric (NCF) consisting of a layer of UD rovings and a backing layer with thin fibers oriented in the in-plane transverse direction. The two layers are held together with stitching and the total nominal thickness is 1 mm. A previous investigation of the shear properties of the fabric material [14] has shown that it primarily deforms in pure shear for the angles relevant for wind turbine blade production as opposed to simple shear, which is typically seen with pure UD fabrics. The pure shear deformation will thus be the kinematic basis for the draping model (described in the next section). Further, it was found that the fabric behaves similarly in positive and negative shear (i.e. direction in which a roving rotate). This means, that e.g. a shear angle of 4° will require the same shear force magnitude to reach as a shear angle of −4°. Regarding the shear limit, a steep increase in the shear force curve was seen at around 25°. Such an increase is usually considered as the limit for forming processes. However, in a production setting with a full-size fabric and boundary conditions that differ from those of the coupon test, it is not certain that such high values of shear can be reached. Experimental testing at the proper process conditions will be necessary; an estimate is a limit of around 10°.

The mold surface tested in this study (see e.g. Fig. 2) was created to resemble a section of a wind turbine blade mold, e.g. to produce a preform. In one end, the surface profile is approximately a circular arc (arc length: 1.67 m, min. radius of curvature: 0.67 m), i.e. stemming from the root part of the blade. In the other end, the surface profile resembles an aerodynamic shape of the blade (arc length: 1.63 m, min. radius of curvature: 0.22 m). The two surface profiles are 4 m apart and connected by linear interpolation and this transition creates a ruled surface with double curvatures. These surface profiles and their connections constitute the *net boundary*, i.e. inside which the fabric material must be placed. The mold surface is then extrapolated to the *extended boundary* to facilitate draping of complete courses. Fabric material located outside of the net boundary after draping must be trimmed. The mold surface files are available on a repository [15].

2.2. The kinematic draping model

For many years, the use of kinematics to predict the final draped configuration of a fabric on a double-curved mold has been employed [16,17]. In doing so it is assumed, as previously stated, that the roving extensional stiffness is infinite and the shear stiffness is negligible. In addition, the in-plane bending stiffness of the rovings is not accounted for, and nor is the possibility of slippage of the rovings with respect to the stitches. With these assumptions, the fabric can be modeled as a grid of nodes that can be placed on the double-curved mold surface.

In this study, rectangular fabrics are considered. An in-house MATLAB code was developed, which is available on a repository [15]. It builds upon a previously published 99-line simple implementation [18,19]. The algorithm relies on first creating a pair of *generators*, i.e. curves that represent fiber paths which subsequently can be populated with nodes. The two generators will intersect at the *origin node*. The generator nodes will form a row and column of the draping grid respectively and will thereby constrain the draping pattern to a unique solution. After the specification of generators, the remaining constrained nodes can be placed. A partially draped course with generators is sketched in Fig. 1.

The lengthwise generator nodes are placed along a *steering curve*, i.e. a parameterized curve which can be used to control the course placement (an update to the simple implementation). A natural cubic spline is used to form the steering curve to ensure smoothness, and its control points can be determined through the optimization routine. In the widthwise course direction, a geodesic curve is used as the generator with its starting direction chosen such that it is perpendicular to the steering curve. This condition entails zero shear at the origin node. Compared to the simple draping algorithm implementation, the calculation of geodesic curves has been improved by a more efficient formulation. Basically it is a solution to the initial value geodesic problem, i.e. calculating a geodesic curve from a starting point and direction. The stopping criteria for the curve is a target length. The algorithm behind this calculation relies on iterative unfolding of the triangles of the mold surface mesh to a common plane, such that the geodesic line can be computed as a straight line [20].

The commercial implementations of the kinematic draping models do offer more or less similar algorithms as described above but it was decided to use the in-house code due to more flexibility of controlling the course placement and dimensions, limitations in scriptable interfaces as well as removing the computational overhead from using an external analysis program. Further, a comprehensive optimization library is readily available with MATLAB [21].

The above description has concerned a single course and it will now be described how that works as the building block to model the entire the layup. When multiple courses are draped next to each other, they form a *layer* as e.g. seen in Fig. 2. The courses in a layer will be draped one by one, starting from the right side of the mold (max. x-coordinate), with the next courses being draped to the left of the previous. Notice though that the draping order as well might be from left to right. When multiple layers are draped on top of each other, they form a *stack*. Naturally, the mold surface must be offset in the thickness direction when advancing to a new layer in the stack to compensate for the thickness of the plies in the previous layer. This offsetting is handled by a CAD program and the offset distance is set to the nominal ply thickness of 1 mm. In this study, layers covering the entire mold surface are considered, which means that the thickness offset is the same everywhere on the mold surface. If for instance plies would be dropped in a layer, the offsetting would become non-uniform and depending on the layup. But as long as the layup plan is defined a priori, the offsetting could be done independently of the optimization, without the need for updating. In reality, shearing of the fabric will also result in a thickness increase. This increase can be estimated by assuming conservation of volume (for instance employed in Composites Modeler for Abaqus/CAE [2]). With the assumption, it can be shown with a deforming parallelogram (equivalent to a single draping cell) that e.g. a shear angle of 10° will result in a thickness increase of 1.5%. Based on this number and in the interest of keeping the thickness offsetting independent of the optimization, it was decided to disregard thickness changes due to shearing.

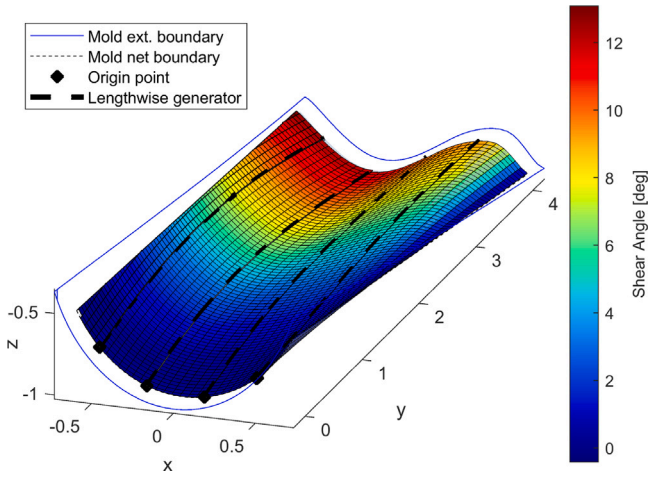

Fig. 2. A single layer with 5 courses of 350 mm width colored based on shear angle (max: 13.1°). The origin nodes are at the start of each course. The first/rightmost course is draped along the right mold net boundary line and the subsequent courses have a 5 mm gap. The leftmost course has been trimmed to the mold net boundary.

Regarding the manufacturing process, it is likewise envisioned that the layup will be created course-by-course as this is expected to give more control of the placement. The actual layup process is, however, outside of the scope of the present investigation.

2.3. Post-evaluation of the structural performance

After a draping analysis has been conducted, the resulting re-oriented fiber angles can be transferred to a structural FE analysis (the definition of fiber angles in the draping model is elaborated in Section 3.2). A different mesh is used to represent the laminate in the FE analysis (structural mesh) than in the draping analysis (draping mesh). Therefore, for each structural element, the closest cell of the draping mesh is located and the corresponding fiber angle stored. The approach was benchmarked against Composites Modeler for Abaqus and the resulting displacements of the FE model were within 0.03%.

In this study, a simple load case on the test mold geometry is used to demonstrate the stiffness response resulting from different ways of draping the plies. The FE model is meshed with quadrilateral shell elements and the layup is offset such that the mold is the bottom surface of the shell. It is subjected to a fixation of x, y, z-displacements of all nodes in the root end ($y = 0$ m). At the far end ($y = 4$ m), all 43 nodes are made rigid as well as each being subjected to a static unit load. An investigation of loads applied to the different degrees of freedom revealed that a y-direction/axial force was most critical when evaluating the impact of the fiber angles on the stiffness, which is thus used in the model. A single draped layer is considered and therefore the thickness is 1 mm. The mechanical properties of the UD ply are listed in Table 1. It was chosen to consider the max. y-displacement or elongation of the model, $U_y^{\max}$ as the measure of mechanical performance as it relates to the stiffness.

The reference for the structural comparisons will be a model in which the fiber angles are not taken from a draping analysis. Instead, the nominal fiber direction, here 0°, is projected onto the element plane. This configuration corresponds to ideal fiber angles, i.e. without draping effects. As an initial comparison, consider the draping result

Table 1
Structural properties of UD plies in FE analysis. The data is for a typical high-modulus glass fiber reinforced polymer for wind turbine blades.

E_1	E_2	ν_{12}	G_{12}	G_{13}	G_{23}
55 GPa	9 GPa	0.3	3.6 GPa	3.6 GPa	3.5 GPa

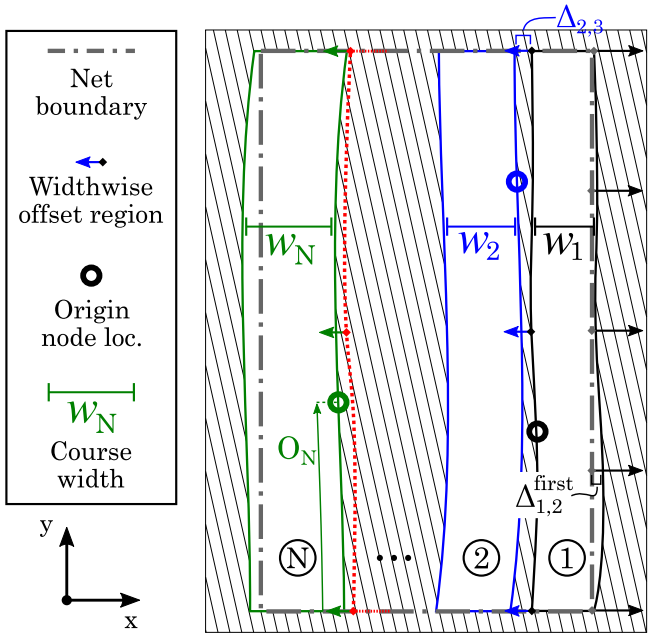

Fig. 3. Parameterization of optimization problem with widthwise offsets, origin node locations and course widths. Each course number is shown enclosed in a circle. The left edge of course $\#N-1$ is visible as the red dotted line. As examples, are indicated the 2nd widthwise offset for course #1, i.e. $\Delta^{\text{first}}_{1,2}$, the 3rd widthwise offset for course #2, i.e. $\Delta_{2,3}$ (top right corner) and also the origin node location for the Nth course, i.e. O_N.

in Fig. 2. As it will become evident in the results section (Section 4) it is not a superior configuration but nonetheless a feasible configuration which can be used as a baseline. With this design, $U_y^{\max}$ increases by approximately 6% compared to the model with ideal fiber angles.

3. Optimization problem

As stated in the introduction, the purpose of the optimization is to take drapability (producibility), structural performance, material waste and practical placement concerns into account. These goals will be achieved through the parameterization of the design and the choice of criteria, which will be described in the following. Lastly, the applied optimization algorithm is described.

3.1. Parameterization

The parameterization is sketched in Fig. 3. As explained previously, the courses in a layer will be draped one by one and their placement is controlled by the steering curve, i.e. lengthwise generator. Rather than specifying the steering curves in absolute coordinates, they are specified relative to a reference curve. The reference curve of the first course is the right mold net boundary line and the subsequent courses use the right edge of the previous course. The actual steering curve is adjusted from the reference curve by means of widthwise offsets. The offsets are introduced at predefined y-coordinates of the reference curve and the offsetting distance is in the x-direction. This simplification of offset handling can be made because the shape of the mold is close to rectangular.

For the first course in a layer, the widthwise offsets are created such that the right course edge can be outside of the net boundary (offset in the positive x-direction), but not inside, as this would mean incomplete mold coverage. There is no physical limit to how much the course can exceed the boundary, but the more it does, the more waste is generated. A maximum value of 150 mm is chosen. Five offsets will be defined along the length of the course, i.e. at 0, 1, 2, 3, and 4 m. The rth widthwise offset of the first course in the kth layer is denoted $\Delta^{\text{first}}_{k,r}$ with $k = 1, \dots, N_{\text{layer}}$ and $r = 1, \dots, 5$. Notice that the double index is merely convenient notation to indicate the structure of the design variables.

For the remaining courses in a layer, the pertaining widthwise offsets can in principle be both positive and negative in x-coordinates. A negative offset means a gap between the courses and a positive offset means an overlap. Due to the shortcomings of the manual layup process a placement tolerance of the courses is normally allowed. In this study, a gap of maximum 12 mm with no overlap is used. With the automatic draping system it is envisioned that the draping can be controlled with much greater accuracy and for this reason the full placement tolerance will be used as the design space for the course placement. The reason why an overlap is not allowed is that it will entail fibers oriented out of plane if e.g. the overlap is varying along the length of the course. Such a situation is likely to result in a knock-down of the laminate strength. Three offsets will be defined along the course length, i.e. at 0, 2, and 4 m. The sth widthwise offset of the mth course is denoted $\Delta_{m,s}$ with $m = 1, \dots, N_{\text{course}} - N_{\text{layer}}$ and $m = 1, \dots, 3$. Here, N_{course} is the number of courses in the stack.

Another design parameter is the origin node in each course. As the origin node defines a location of zero shear, it controls how the shear is distributed in the course. In a manual layup process, the origin node corresponds to the starting point of draping. The origin node is located on the course edge and must be between 0% and 100% of the course length. In the draping algorithm it is handled as a discrete value, i.e. the index in the draping grid. The origin node of the jth course is denoted O_j with $j = 1, \dots, N_{\text{course}}$.

The final design parameter is the width of the courses. The setup is such that the optimizer can select each course width from a pre-defined list of available fabric roll widths, i.e. an integer design variable. The available widths are 350 mm, 400 mm and 450 mm. The width of the jth course is denoted w_j with $j = 1, \dots, N_{\text{course}}$. To ensure that the mold surface is always completely covered within the net boundary, regardless of the chosen widths, a number of courses corresponding to complete coverage with the smallest available width is initialized. After each course is draped, potential trimming is checked, i.e. intersection between the course and the mold net boundary. If the complete length of a course is trimmed, i.e. that the entire course length has crossed the mold net boundary, the draping of the layer in question is terminated. That is, if one or more additional courses were initialized in the layer, they are not draped. In that way, only the necessary number of courses is draped.

The parameterization with design variables of the course optimization is summarized in Table 2.

3.2. Criteria

Three criteria are included in the scalar objective function to be minimized: shear angles, deviations of the UD fiber angles from a target value, and material waste as sketched in Fig. 4.

Minimizing the shear angles will make the draping easier (and potentially faster with an automatic system), because less in-plane deformation of the fabric is required for it to conform to the mold. The shear angle of a cell is defined as the change of angle between the two adjacent cell edges from the initial 90° in the unsheared configuration. Thus, a shear angle is computed for each node in the cell and subsequently, the four cell values are averaged for use in the optimization. The computation is done in the plane of the cell using the 3D vectors that form the cell edges.

Table 2
Overview of design variables in the course optimization.

	Description	Type	Range
$\Delta_{k,r}^{\text{first}}$	Widthwise offset of 1st course in layer	Continuous	Up to 150 mm outside net boundary
$\Delta_{m,s}$	Widthwise offset between remaining courses	Continuous	Up to 12 mm gap
O_j	Origin node location (grid index)	Discrete	From 1 to the number of lengthwise grid nodes
w_j	Width of course	Discrete	350 mm/400 mm/450 mm

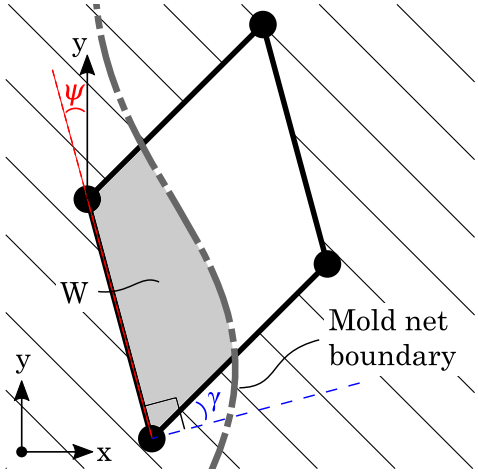

Fig. 4. Single draping cell on the mold surface with indication of shear angle (γ), UD fiber angle (ψ) and material waste (W, solid gray area).

The fiber angles govern the mechanical properties of the laminate and during the structural design, fiber plies with certain orientations are carefully specified according to the load cases to which the structure will be subjected in service. But with a general double-curved mold and the nature of fabrics, it is not possible to have fiber angles at every location in the stack matching an ideal global direction. That is, there will be fiber angle deviations due to the draping effects. Minimizing these deviations will therefore improve the mechanical properties of the laminate. Including the fiber angle deviations in the objective function is much more efficient than including the stiffness response from the FE model directly in the optimization, i.e. running an FE analysis for each function evaluation in the optimization. In this study, the UD fiber angle is defined as the angle between a lengthwise cell edge and the global y-axis, i.e. with one unique value for each cell. The computation is done by projecting the global y-axis onto the plane of the cell and computing the angle between the projection and the lengthwise cell edge. Because the target value of the UD fiber angles is 0°, the criteria will henceforth simply be referred to as minimization of UD fiber angles. Notice that both the shear angles and UD fiber angles are signed.

Lastly, minimizing the material waste will save costs for raw material as well as making the manufacturing process more sustainable. The material waste of a cell is defined as the cell area that is outside of the mold net boundary after draping. Whether the material is trimmed before or after draping in a production setting is irrelevant, because it will have to be cut from a fabric roll of a certain width.

These three, potentially conflicting, criteria must be handled by the optimization algorithm. To make the formulation as generally applicable as possible, it was decided to use a single-objective weighted sum formulation. This means adding the three criteria multiplied by suitable weight factors, to obtain a combined scalar objective function. The topic of a multi-objective formulation is revisited in the discussion (Section 5).

Both shear angles and UD fiber angles are field quantities and for this reason a p-norm function is used to aggregate each of them into a scalar quantity. The p-norm function is a continuous approximation

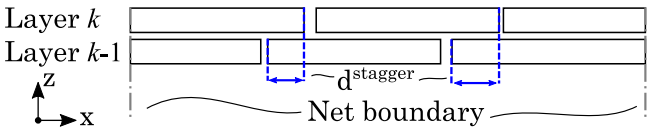

Fig. 5. Definition of stagger distance, d^{stagger}, between adjacent layers.

of the maximum value. The angles are first aggregated for each layer, here exemplified with the variable α:

$$\|\alpha\|_p^{\text{layer},k} = \left(\sum_{i=1}^{N_\alpha} |\alpha_{i,k}|^p \right)^{\left(\frac{1}{p}\right)} \tag{1}$$

Here $\alpha_{i,k}$ signifies the ith angle quantity of the kth layer to be aggregated and N_α is the number of angle values, i.e. the number of cells in the layer. When computing the objective function for a stack of multiple layers, the layerwise values are averaged:

$$\overline{\|\alpha\|_p^{\text{layer}}} = \frac{1}{N_{\text{layer}}} \sum_{k=1}^{N_{\text{layer}}} \|\alpha\|_p^{\text{layer},k} \tag{2}$$

N_{layer} denotes the number of layers. This layer-averaging has the advantage of evening out the contributions from the different layers to the objective function as well as avoiding a behavior change of the p-norm function due to an increase in the number of aggregated values. For shear angles, mainly the maximum absolute value is of interest because it will be the limiting factor for draping. For this reason, it is chosen to use $p = \infty$ for shear angle aggregation. Notice though, that this merely is the mathematical basis, and it is implemented using the max function to avoid numerical problems. For the UD fiber angles, the distribution of angles also matter because the mechanical response of the composite part will be influenced by the fiber angle at every point in the laminate. Here, $p = 6$ is chosen, because it approximates the maximum value but still has contributions from the lower values. Therefore, the two means of the aggregated field quantities can readily be added in the objective function because they have the same unit of degrees as well as the same order of magnitude.

The material waste of the kth layer, $W^{\text{layer},k}$ is a scalar arising from summing the contributions from all cells in the layer, but it does not have the same order of magnitude and can therefore not be added directly in the objective function. For this reason the waste term is scaled by choosing values of the material waste and shear angles, $W_{\text{layer}}^{\text{eq}}$ and γ^{eq}, that have a similar impact on the design:

$$W_{\text{scaled}}^{\text{layer},k} = \gamma_{\text{eq}} \frac{W^{\text{layer},k}}{W_{\text{eq}}^{\text{layer}}} \tag{3}$$

Effectively the scaling works like a weighted sum formulation, but with a physical interpretation of the weight. The values are chosen to $\gamma_{\text{eq}} = 6°$ and $W_{\text{eq}}^{\text{layer}} = 0.4\ \text{m}^2$, i.e. corresponding to 25% of the area of a 400 mm wide course. The waste from each layer is likewise averaged for the stack objective function.

A single family of nonlinear constraints is also included in the optimization. The purpose is to enforce a reasonable staggering of the courses when draping a new layer as sketched in Fig. 5. If the course edges from two adjacent layers are too close to each other the high resin content in that region will weaken the laminate. The principle is the same as when building a brick wall. The number of stagger distance

Table 3
Settings for genetic algorithm. The different reproduction operators are the default settings.

Parameter	Setting
Population size	100 per layer
Elite count	5 per layer
Crossover children[a]	76 per layer
Mutation children	19 per layer
Max. generations	100 per layer
Function tolerance	1×10^{-6}
Stall generations	40 per layer
Crossover operator	Laplace
Mutation operator	Power
Parent selection operator	Tournament

[a]The number of crossover and mutation children is based on a crossover fraction setting of 0.8.

constraints, N_{stagger} depends on the number of courses in each layer and the total number of layers. For layers $\#2, \ldots, N_{\text{layer}}$ a constraint is defined for the left and right edges of each course, except for the rightmost and leftmost as those define the edges of the stack, i.e. at the net boundary. A stagger distance for a particular course edge is calculated as the minimum distance from any node of that course edge to any edge node of all courses in the previous layer. The minimum distance of d^{stagger} is set to 20 mm.

Basically, all criteria are influenced by all design parameters although the coupling between some is stronger than with others. For instance, the width of the courses has a strong impact on the amount of waste generated as well as the staggering but also potentially the shear as a wider course means more material in which the shear can propagate and increase. The origin node location has a strong impact on the shear distribution but as a course becomes narrower when it shears, it also has a minor, probably negligible, impact on waste and staggering. Shear and fiber angle deviations can develop from both conformation to double curvatures as well as course steering. The latter is controlled by the widthwise offsets which can thus "straighten out" a course. This steering curve manipulation can reduce shear and fiber angle deviations but also has a direct impact on waste and staggering.

3.3. Formulation

The problem of determining the optimal course placement for a stack is implemented in two ways:

1. Optimization with all layers at the same time.
2. Sequential optimization with one layer at the time.

The former will have a higher number of design variables compared to each sequential problem of the latter. Due to the scaling nature of optimization problems, it is expected that the sequential approach will be faster overall. For a given layer in the sequential approach, the course edges from underlying layers must be input so that staggering can be taken into account. The question is, if a feasible solution can always be found with this approach.

The design variables of the problem are stored in the vector **a**. It consists of the widthwise offsets of the first course in each layer (draped relative to the right net boundary line), the widthwise offsets of the remaining courses (draped relative to the previous course), the origin node locations, and the course widths (refer to Fig. 3 and Table 2):

$$\mathbf{a} = \left[\boldsymbol{\Delta}^{\mathbf{first}}, \boldsymbol{\Delta}, \mathbf{O}, \mathbf{w}\right] \tag{4}$$

The optimization problem in the classical form, is written as follows:

$$\begin{aligned}
\underset{\mathbf{a}}{\text{minimize}} \quad & \overline{\|\gamma\|_{p=\infty}^{\text{layer}}} + \overline{\|\psi\|_{p=6}^{\text{layer}}} + \overline{W_{\text{scaled}}^{\text{stack}}} \\
\text{s.t.} \quad & (1) \quad d_n^{\text{stagger}} \geq 20\,\text{mm} \\
& (2) \quad 0\,\text{mm} \leq \Delta_{k,r}^{\text{first}} \leq 150\,\text{mm} \\
& (3) \quad -12\,\text{mm} \leq \Delta_{\text{m,s}} \leq 0\,\text{mm} \\
& (4) \quad 0\% \leq O_j \leq 100\% \\
& (5) \quad w_j \in \{350\,\text{mm}, 400\,\text{mm}, 450\,\text{mm}\}
\end{aligned} \tag{5}$$

$$\begin{aligned}
&\forall n = 1, \ldots, N_{\text{stagger}} \quad , \forall m = 1, \ldots, N_{\text{course}} - N_{\text{layer}} \\
&, \forall j = 1, \ldots, N_{\text{course}} \quad , \forall k = 1, \ldots, N_{\text{layer}} \\
&, \forall r = 1, \ldots, 5 \quad , \forall s = 1, \ldots, 3
\end{aligned}$$

The objective function is the sum of the three quantities explained in Fig. 4, i.e. the layerwise mean of the aggregated shear angles, the layerwise mean of aggregated UD fiber angles and the layerwise mean of the scaled material waste. The first constraint (1) concerns the stagger distances and the remaining constraints (2)–(5) are the bounds on the design variables.

3.4. Optimization algorithm

The reviewed references in the beginning of this paper that concern draping optimization mostly make use of zero-order or derivative-free optimization methods. The reason is the highly nonlinear nature of the problem with multiple local minima as well as the integer constraints. In this study the Genetic Algorithm (GA) implemented in MATLAB will be applied as the expectation is that it will converge to better minima than a gradient-based method.

The idea behind the algorithm is to mimic the process of natural selection. An important part of the algorithm is the generation of random numbers and here, the default *Mersenne twister* generator is employed. In brief, the GA works with a *population* in each iteration, i.e. a set of different designs. Each individual in the population is basically represented by a vector of design variables. First, a random, initial population is generated. For each individual in the population, the fitness (objective function) value to be minimized is evaluated. The next population, i.e. the next iteration designs, is composed of three different parts: (1) Elite: some of the individuals with the lowest fitness scores are passed on directly. (2) Crossover: *children* are created by combining the vector entries from a pair of *parents*, i.e. individuals of the current population. (3) Mutation: Children are created by random changes to a single parent. Nonlinear constraints are handled by means of a penalty algorithm that increases the fitness function of an individual e.g. by adding the sum of constraint violations. The creation of new populations continues until one of the stopping criteria is met [21]. These criteria are the maximum number of generations (set to 100 per layer) and a tolerance on the average change of the fitness function value (set to 1e-6) over a set number of *stall generations* (set to 40 per layer). The settings used for the genetic algorithm can be found in Table 3. See also the MATLAB Global Optimization Toolbox documentation page [21] for more information.

In the MATLAB implementation, the generation of designs can be parallelized onto multiple cores. In this study, a workstation with a 32 core AMD EPYC 7302 processor (2.99 GHz) is used to greatly speed up the optimization.

4. Results

Optimization results with the test mold are presented in this section. Three different setups are considered:

1. Single-layer unconstrained model highlighting the effect of the different criteria in the objective function, Eq. (5). The structural performance, i.e. max. elongation, Uy^{max}, will also be evaluated. The four cases considered are:
   (a) Only shear angles, γ.
   (b) Only UD fiber angles, ψ.
   (c) Only material waste, W.

Table 4
Results of single layer optimization with different criteria. The columns are the min., max. and average values of, respectively, shear angles and UD fiber angles, the total waste and the elongation of the FE model with draped fiber angles relative to the model with projected/ideal fiber angles.

	Shear angles			UD fiber angles			Waste	Elongation
	$\gamma_{\min}$ [°]	$\gamma_{\max}$ [°]	γ_{avg} [°]	$\psi_{\min}$ [°]	$\psi_{\max}$ [°]	ψ_{avg} [°]	W^{stack} [m^2]	Rel. $Uy^{\max}$ [%]
Baseline (Fig. 2)	−0.42	13.10	4.09	−7.91	4.89	−0.07	0.68	5.95
(a), min γ	**−2.72**	**2.70**	**−0.41**	−3.22	4.20	0.58	0.37	1.30
(b), min ψ	−1.27	12.34	0.28	**−1.44**	**3.46**	**−0.18**	1.00	0.36
(c), min W	−5.24	3.19	−0.08	−3.14	4.77	−0.08	**0.10**	1.15
(d), min $\gamma+\psi+W$	**−3.55**	**3.32**	**−0.19**	**−2.00**	**3.45**	**−0.23**	**0.13**	0.68

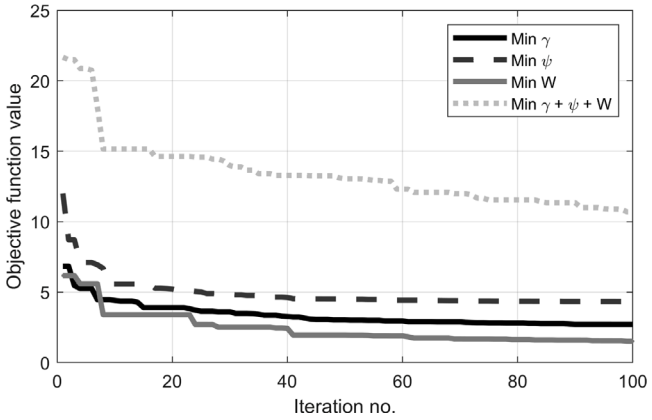

Fig. 6. Convergence history of the single-layer results.

(d) All three criteria together, $\gamma+\psi+W$.

2. 5-layer model including nonlinear stagger distance constraints. The thickness offset between each layer is 20 mm, i.e. corresponding to 20 nominal ply thicknesses. This setup serves to show the effects of layer offsetting as well as testing the two different implementations described in Section 3.3, i.e.:

   (a) Optimizing all layers at the same time.
   (b) Optimizing the layers sequentially.

3. 30-layer model including nonlinear stagger distance constraints. The thickness offset between each layer is 1 mm. This setup serves to illustrate that a full-scale industry-relevant model can be handled.

All results have been selected as the best of three runs with different seeds of the random number generator, i.e. 0,1,2. Although a function tolerance was specified as stopping criteria, all feasible solutions stopped due to reaching the maximum number of generations. All feasible optimization runs exhibited monotonic convergence. Details of the design variables for the single-layer optimization is given in Appendix and for the remaining results as electronic supplementary material.

4.1. Single-layer optimization

The results of the single layer optimization are presented graphically in Fig. 7 and selected data can be found in Table 4 together with data from the baseline design in Fig. 2. For both shear angles and UD fiber angles, the four optimized designs are improvements over the baseline design. The main drivers for these improvements are the possibility of the 1st course in the layer to exceed the right net boundary line to straighten out the course (not applied in the baseline design) as well as manipulated origin node locations (all at 0% course length in the baseline design). Due to the improvements of the UD fiber angles in the optimized designs, the respective $Uy^{\max}$ relative to the model with projected fiber angles are also significantly lower than for the baseline design. So low, in fact, that the necessity of including the draped fiber angles in a structural analysis in this example is debatable. This topic will be revisited in the discussion (Section 5).

Table 5
Results of 5-layer optimization. The columns are the maximum absolute shear angles, the average UD fiber angles, the standard deviation of the UD fiber angles and waste.

		max(|γ|) [°]	$\overline{\psi}$ [°]	std(ψ) [°]	W [m^2]
All-layer	L #1	3.23	0.27	0.85	0.60
	L #2	4.33	−0.19	0.83	0.25
	L #3	4.12	0.24	0.90	0.73
	L #4	4.76	−0.52	0.87	0.28
	L #5	5.42	−0.54	0.85	0.32
	Stack	5.42	−0.14	0.93	2.18
Seq.	L #1	3.55	−0.23	0.94	0.13
	L #2	4.07	−0.24	0.76	0.26
	L #3	4.63	−0.18	0.83	0.29
	L #4	4.62	−0.39	0.74	0.47
	L #5	6.52	−0.88	0.65	0.51
	Stack	6.52	−0.38	0.83	1.65

As stated in the introduction of the section, the convergence was monotonic, which can be seen in the convergence plot in Fig. 6. All optimization runs were terminated due to reaching the maximum number of generations (100) and all used a total of 9605 function evaluations.

It is also worth to note that for each of the three single-optimization setups, the criteria that is minimized does in fact have the lowest value when considering all the optimization runs. E.g. case (a) with minimization of shear does have the overall lowest value of the maximum absolute shear angle, i.e. 2.70°. Further, case (b) with minimization of UD fiber angles does have the tightest distribution around 0° in the histogram. Overall, the results with all three criteria in case (d) seem to be a good compromise. It will thus be used for the subsequent setups.

4.2. 5-layer optimization

The best result from the 5-layer optimization is presented graphically in Fig. 8 with supporting data available in Table 5. Based on the findings of the single-layer optimization, it was decided to report the maximum absolute shear angle, respectively, the average and standard deviation of the UD fiber angles, and the waste.

Recall, that two formulations were tested. The first is all layers optimized at the same time, which is a single run of 500 iterations with population size 500. The second is the sequential layer formulation with five runs, i.e. one for each layer, of an optimization with 100 iterations and population size 100. As expected, the sequential formulation is significantly faster than the all-layer formulation. On average, the former only took 1.5 h (48,520 function evaluations), whereas the latter took 33.7 h to complete (250,500 function evaluations). This is a reduction of almost 96%. In fact, the sequential optimization could be completed with 500 iterations per layer in less than the time used for the total 500 iterations with the all-layer formulation.

Comparing the objective function values of the two formulations, the difference is less than 10% in favor of the sequential formulation.

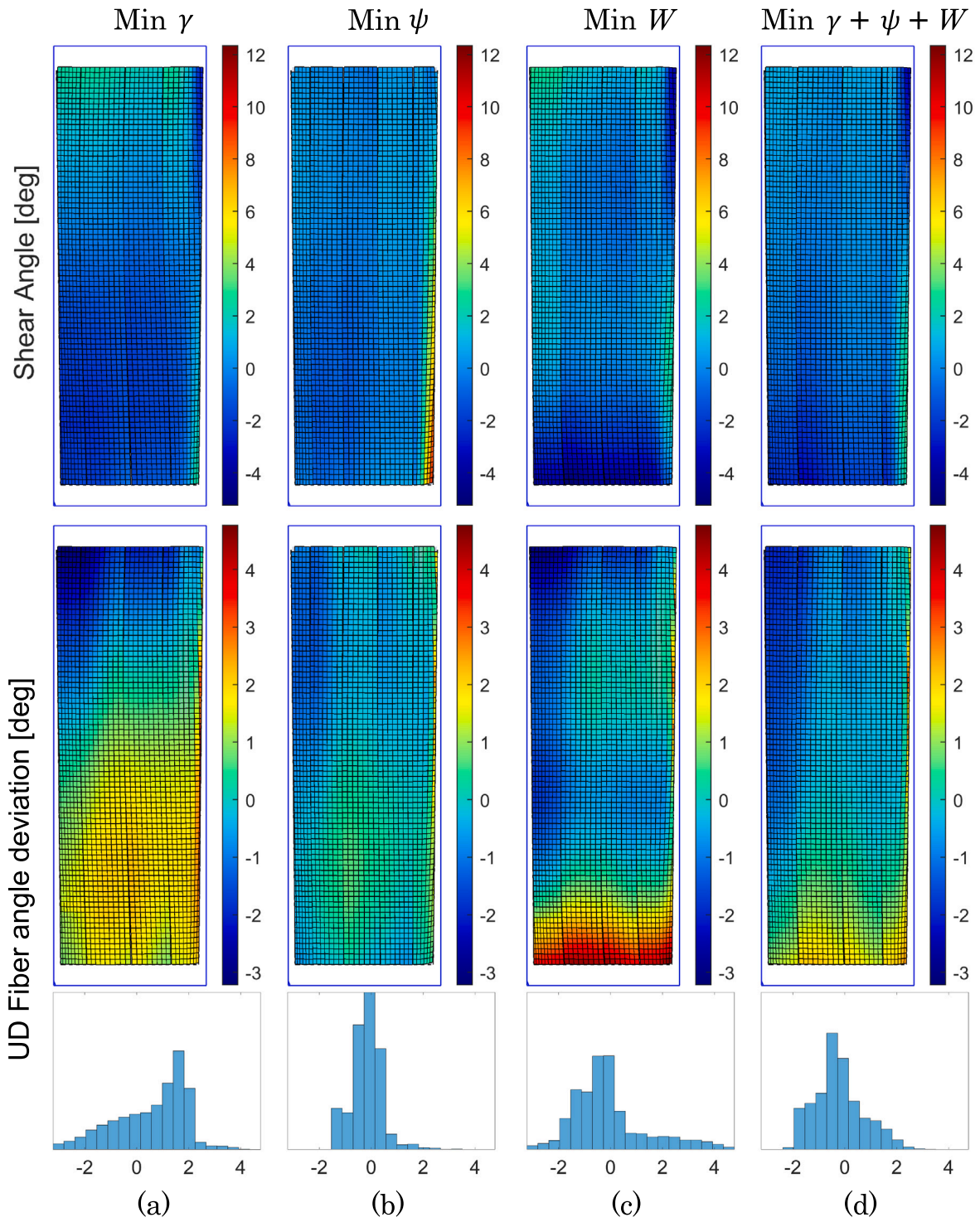

Fig. 7. Top view results from single layer optimization with different criteria visualized as shear angles and UD fiber angles including a histogram: (a) Min. shear angles, (b) Min. UD fiber angles (c) Min. material waste, and (d) Min. shear angles, UD fiber angles and material waste.

From Table 5 it is also clear that the two results are close. While the shear angles of the sequential formulation are slightly inferior to those of the all-layer formulation, the standard deviations of the UD fiber angles are lower and the total waste is reduced by 24%. These results are a consequence of the composition of the objective function (defined in Section 3.2), which is a point discussed in Section 5.

The result presented in Fig. 8 is thus from the sequential formulation. Comparing the shear distribution in Fig. 8(a) to that of the single-layer result in Fig. 7(d), it can be seen that the tendency is the same: the rightmost course has the highest shear angles and the remaining courses have lower shear angles. In the flattened stack plot in Fig. 8(b) the staggering at the root end can be seen. Notice that the widthwise mold arc length decreases with increasing layer number. All three runs, i.e. with different seeds, of the sequential formulation yielded feasible solutions with a minimum stagger distance of 20 mm. For the all-layer formulation one of the three runs ended up infeasible. Apart from the random number generator seed, different settings for the optimization algorithm could influence this infeasibility.

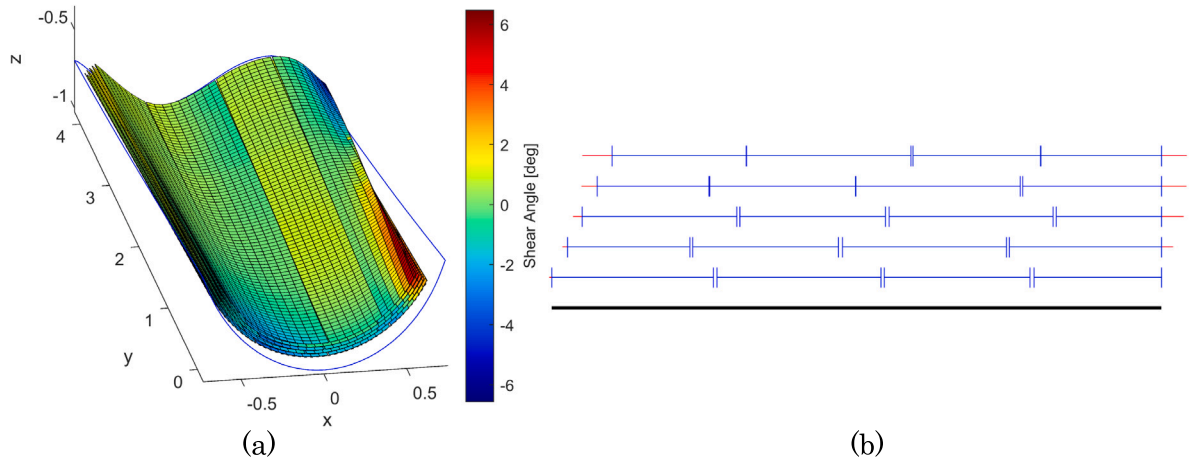

Fig. 8. Draped results from sequential 5-layer optimization. (a) Draped courses colored based on shear angles. (b) Flattened stack plot at the root end. The lower black line represents the mold surface. The courses are represented by blue lines with their ends indicated by the vertical bars. Trimmed-off parts are colored in red.

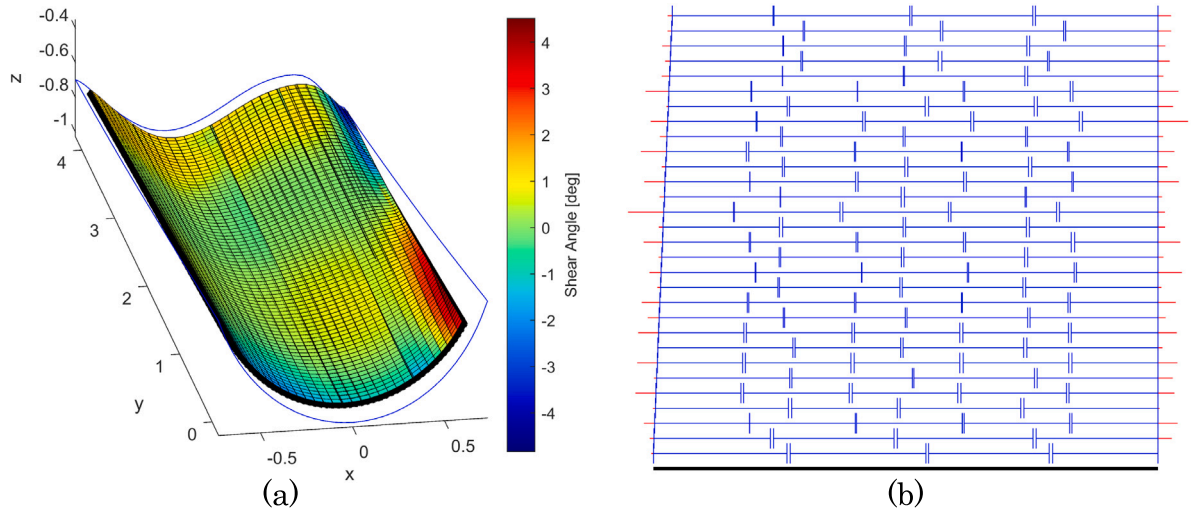

Fig. 9. Draped results from sequential 30-layer optimization. (a) Draped courses colored based on shear angles. (b) Flattened stack plot at the root end. The lower black line represents the mold surface. The courses are represented by blue lines with their ends indicated by the vertical bars. Trimmed-off parts are colored in red.

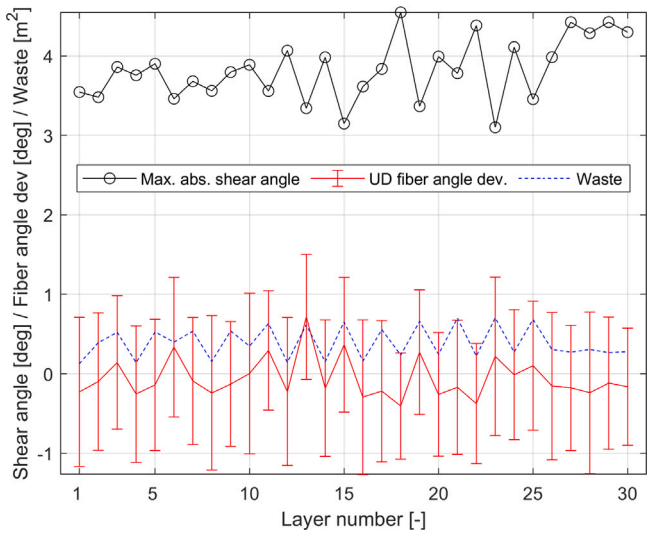

Fig. 10. Layer-wise results from 30-layer optimization indicating the maximum absolute shear angle, the mean and standard deviation (error bars) of the UD fiber angles and the waste.

There is a general tendency that the shear angles and UD fiber angle deviations increase with layer number. This increase is due to the fact that the mold curvatures increase because of the layer offsetting. There is no general tendency in terms of the waste but here it should be kept in mind that the widthwise mold arc lengths change due to the layer offsetting. For this reason, minimizing waste in one layer could be easier to achieve than in another layer, because the same course widths are available.

4.3. 30-layer optimization

With the findings from the 5-layer optimization, it was decided to use the sequential formulation for the 30-layer optimization. The result with the lowest objective function is presented in Fig. 9 and selected supporting data are plotted layer-wise in Fig. 10 as the maximum absolute shear angle, the mean and standard deviation of the UD fiber angles and the waste.

Again, the shear angle plot in Fig. 9(a) is similar in tendency to both the single-layer result in Fig. 7(d) and the 5-layer result in Fig. 9(a). Offset-wise, the top layer of the 30-layer model is halfway between the 2nd and 3rd layer of the 5-layer model and from Table 5, it can be seen that the shear angles are comparable in magnitude. The staggering at the root end can be seen in Fig. 10(b). Of the three runs with different

seeds for the random number generator, one had an infeasible layer, which thus unfortunately rendered the entire stack infeasible. Recall that the current approach is to run all the layers with the same seed. To this end, it could be interesting to run each layer with the different seeds, pick the best result, continue to the next layer, run with the different seeds etc.

The layer-wise results in Fig. 10 are fairly stable over the course of the layers. From the figure it seems that the different criteria balance each other. Consider e.g. layer #18, which has the highest maximum absolute shear angle in the stack of 4.55°. The same layer also has the lowest standard deviation of the UD fiber angles of 0.67°.

The average run-time for this setup was approximately 9.5 h (288,645 function evaluations) or 0.32 h per layer. Comparing this run-time to that of the 5-layer optimization (on average 0.30 h per layer), it can be concluded that the scaling is approximately linear in the number of layers. This is very useful information because the required optimization time for larger models can be predicted reasonably well from running smaller models.

5. Discussion

The results from the previous section have demonstrated the applicability of the presented method: The starting point was an already defined overall UD layup and the outcome is the specification of the individual courses (width and placement) taking the shear angles, UD fiber angle deviations, waste and staggering into account. The use of the UD fiber angle deviations as a criterion for mechanical performance was shown to be a valid approximation in the presented examples. That is, the result with the lowest value of fiber angle deviations, also had the lowest elongation when simulated with an FE analysis.

The next logical step will be to create a coupling back to the structural design process. This step was briefly exemplified in the paper with the "structural post-evaluation"-step, but all the pertaining failure criteria should be evaluated for the as-manufactured design. Possibly, it could be necessary to iterate the process. Another applicability is, if for instance an optimization procedure is used to specify the structural design like in the Discrete Material and Thickness Optimization approach, see e.g. [22]. Here, the outer laminate geometry could be fixed and using a number of predefined *candidate materials*, e.g. UD, biaxial and core material, the optimizer can decide the best layup. The laminate will typically be divided into a number of patches with constant layup. In this case, the methodology presented in this paper could be used to generate the database of updated/feasible candidate materials for the different patches [10]. That is, if the optimizer selects a nominal UD ply for a layer in a certain patch, the structural calculations will use the re-oriented fiber angles from the a priori course draping optimization. In this way, the structural optimization can take the draping process and other related manufacturing constraints into account. In the analyses presented in this paper, a global nominal fiber angle was used as the target. This approach could be extended with multiple local target fiber angles, i.e. in different regions of the mold. Such an extension would enable the creation of a *variable stiffness composite* known from automated fiber placement [23]. The local target angles could for instance follow the principal stress directions to further increase the stiffness of the structure. In regard to stiffness, in Table 4, the relative elongation differences between the models with draped fiber angles and the reference model with projected fiber angles, i.e. Rel. $Uy^{\max}$, were compared. The presented differences are not huge. Nonetheless, eliminating uncertainties from a model is always preferable. Also, as seen from the presented results, the draping effects tend to increase when the stack builds up due to the increasing curvatures. For this reason, larger UD fiber angle deviations could be expected when there are many layers present. Further, it should be noted that with increasing fiber stiffness, the sensitivity of the laminate to fiber re-orientations increases. For example, if the laminate was made with carbon fiber, e.g. with $E_1 = 130$ GPa in Table 1, the relative $Uy^{\max}$ of the baseline design in Fig. 2 increases from the current 6% to more than 15%. The relative $Uy^{\max}$ of the other designs with draped fiber angles in Table 4 increase correspondingly.

If realistic data are available from a real production setting, the objective function could also include cost as also employed by Kaufmann et al. [10]. The current approach with considering the waste in the form of area could be augmented with the length of the cut as this would directly translate to operating time. Further, the number of courses or the total length of the draped courses could also be included as this would likewise be directly relatable to operating time. Another change to the optimization criteria could be to include a maximum shear angle (shear limit) as a constraint and then consider different weightings between the UD fiber angles and the waste. With a dedicated multi-objective optimization algorithm, the objective function can be input as a vector of criteria. Thereby, the *Pareto front* could be mapped, thus presenting the trade-off between the two criteria.

The introduction of gaps (and potentially overlaps) between the courses will likely result in a knock-down of the mechanical performance. This knock-down must, however, be weighed against the potential improvements regarding drapability, waste and possibly mechanical performance due to better fiber alignment. A further detailed investigation will be necessary to characterize this balance.

The presented results in the paper should be viewed in light of the inherent variability of the raw materials as well as process-induced variability. In this case, the variability particularly concerns the fiber angles. The as-delivered glass fiber fabric might not have the fibers perfectly aligned with the specification and depending on the processes for draping, infusion and curing, different kinds of defects could develop [24]. The kinematic draping model employed takes the draping effects into account, but otherwise assumes ideal forming behavior. Experimental investigations and the inclusion of fiber misalignments in the structural models could clarify this matter further.

6. Conclusion

This paper has presented a methodology for generating manufacturing instructions, i.e. specification of the individual fabric courses, from a structural layup plan of a wind turbine blade. In this context a course is defined as a roll-width of fabric of which multiple are necessary to achieve full mold coverage due to the size of the mold. In the study a test mold with a pre-defined layup of overall UD layers is used as the starting point.

Using a parameterized kinematic draping model and a genetic algorithm for optimization, the courses are placed such that the shear angles, deviations of the UD fiber angles from a nominal value and trim-off are minimized. With multiple layers in a stack, stagger distance constraints are introduced such that course edges will not be on top of each other in adjacent layers, which would otherwise weaken the laminate. The design variables concern the placement of the courses on the mold by specifying offsets relative to e.g. the mold net boundary or adjacent courses, the width of the courses and the location of zero shear on the course.

Through the single-layer optimization, the effects of the individual criteria were demonstrated. By transferring the draped fiber angles to structural finite element analyses, it was further illustrated how the stiffness of the model was affected by the different criteria by considering a simple load case.

The 5-layer and 30-layer models showed the applicability of the model and its relevance for industrial applications. By optimizing the layers sequentially, the total optimization time scales approximately linearly with the number of layers. The methodology is completely generic and will work with any smooth mold surface and layup plan, e.g. with dropped layers. With an automatic draping system, the output can be converted to machine settings. The method is an enhancement of the link between design and manufacturing of wind turbine blades which can hopefully aid in lowering the expenses of clean wind energy.

Table A.6
Single-layer design variables from minimization of shear angles.

	OrgNode [%]	Trans. offset [mm]					Width [mm]
Course #1	60.00	52.08	81.63	87.59	61.49	10.74	450
Course #2	70.00	−10.78	−1.59	−8.90	N/A	N/A	400
Course #3	65.00	−11.83	−0.66	−9.46	N/A	N/A	450
Course #4	63.75	−7.49	−5.44	−8.60	N/A	N/A	400

Table A.7
Single-layer design variables from minimization of UD fiber angles.

	OrgNode [%]	Trans. offset [mm]					Width [mm]
Course #1	100.00	35.32	92.08	124.78	116.95	60.49	350
Course #2	35.00	−7.71	−0.17	−11.44	N/A	N/A	350
Course #3	68.75	−5.19	−0.20	−11.92	N/A	N/A	350
Course #4	61.25	−4.18	−0.15	−10.02	N/A	N/A	350
Course #5	50.00	−0.99	−2.71	−11.70	N/A	N/A	450

Table A.8
Single-layer design variables from minimization of waste/trim-off.

	OrgNode [%]	Trans. offset [mm]					Width [mm]
Course #1	58.75	0.45	31.07	75.27	59.59	4.41	450
Course #2	28.75	−10.96	−0.91	−8.99	N/A	N/A	350
Course #3	52.50	−7.09	−0.56	−8.17	N/A	N/A	400
Course #4	21.25	−9.49	−2.02	−2.95	N/A	N/A	450

Table A.9
Single-layer design variables from minimization of shear angles, UD fiber angles and waste/trim-off.

	OrgNode [%]	Trans. offset [mm]					Width [mm]
Course #1	67.50	0.36	43.20	79.10	70.05	15.75	350.00
Course #2	33.75	−10.82	−1.00	−7.81	N/A	N/A	400.00
Course #3	68.75	−8.69	−0.05	−9.54	N/A	N/A	450.00
Course #4	50.00	−10.46	−1.94	−11.11	N/A	N/A	450.00

Funding

This study was completed as part of the MADEBLADES research project supported by the Energy Technology Development and Demonstration Program, Grant no. 64019-0514.

CRediT authorship contribution statement

Christian Krogh: Conceptualization, Methodology, Software, Investigation, Writing – original draft. **Sebastian M. Hermansen:** Conceptualization, Methodology, Writing – review & editing. **Erik Lund:** Conceptualization, Methodology, Writing – review & editing. **Jørgen Kepler:** Conceptualization, Methodology, Writing – review & editing, Supervision. **Johnny Jakobsen:** Conceptualization, Methodology, Writing – review & editing, Supervision.

Declaration of competing interest

The authors declare that they have no known competing financial interests or personal relationships that could have appeared to influence the work reported in this paper.

Data availability

The code and the input data including the mold used for generating the results in this study is available at the repository [15]. Electronic supplementary material of the presented results are available at: http://dx.doi.org/10.17632/3mh3ghrz67.

Appendix. Single-layer design variables

The design variables of the single-layer results presented in Section 4.1 are available in Tables A.6–A.9.

References

[1] Wang J, Paton R, Page JR. Draping of woven fabric preforms and prepregs for production of polymer composite components. Composites A 1999;30(6):757–65. http://dx.doi.org/10.1016/S1359-835X(98)00187-0.

[2] Dassault Systèmes. Composites modeler for abaqus/CAE. 2020, URL https://www.3ds.com/products-services/simulia/products/abaqus/add-ons/composites-modeler-for-abaquscae/.

[3] Ansys Inc. Ansys mechanical. 2020, URL https://www.ansys.com/products/structures/ansys-mechanical.

[4] Siemens Industry Software Inc. Fibersim. 2020, URL https://www.plm.automation.siemens.com/global/en/products/nx/fibersim.html.

[5] Cao J, Akkerman R, Boisse P, Chen J, Cheng HS, de Graaf EF, et al. Characterization of mechanical behavior of woven fabrics: Experimental methods and benchmark results. Composites A 2008;39(6):1037–53. http://dx.doi.org/10.1016/j.compositesa.2008.02.016.

[6] Liang B, Boisse P. A review of numerical analyses and experimental characterization methods for forming of textile reinforcements. Chin J Aeronaut 2021;34(8):143–63. http://dx.doi.org/10.1016/j.cja.2020.09.027.

[7] Fetfatsidis KA, Sherwood JA. Process simulations for predicting quality of composite wind turbine blades. In: Attaf B, editor. Recent advances in composite materials for wind turbine blades. World Academic Publishing; 2013.

[8] Skordos AA, Sutcliffe MPF, Klintworth JW, Adolfsson P. Multi-objective optimisation of woven composite draping using genetic algorithms. In: 27th international conference SAMPE EUROPE. 2006.

[9] Weiland F, Weimer C, Dumont F, Katsiropoulos CV, Pantelakis SG, Sitaras I, et al. Process and cost modelling applied to manufacture of complex aerospace composite part. Plast Rubber Compos 2013;42(10):427–36. http://dx.doi.org/10.1179/1743289812Y.0000000047.

[10] Kaufmann M, Zenkert D, Åkermo M. Cost/weight optimization of composite prepreg structures for best draping strategy. Composites A 2010;41(4):464–72. http://dx.doi.org/10.1016/j.compositesa.2009.11.012.

[11] Köke H, Weiß L, Hühne C, Sinapius M. A graph-based method for calculating draping strategies for the application of fiber-reinforced materials on arbitrary surfaces. Compos Struct 2017;162:123–32. http://dx.doi.org/10.1016/j.compstruct.2016.11.024.

[12] Fengler B, Hrymak A, Kärger L. Multi-objective CoFRP patch optimization with consideration of manufacturing constraints and integrated warpage simulation. Compos Struct 2019;221:110861. http://dx.doi.org/10.1016/j.compstruct.2019.04.033.

[13] Kussmaul R, Jónasson JG, Zogg M, Ermanni P. A novel computational framework for structural optimization with patched laminates. Struct Multidiscip Optim 2019;60(5):2073–91. http://dx.doi.org/10.1007/s00158-019-02311-w.
[14] Krogh C, Kepler JA, Jakobsen J. Pure and simple: investigating the in-plane shear kinematics of a quasi-unidirectional glass fiber non-crimp fabric using the bias-extension test. Int J Mater Form 2021;14(6):1483–95. http://dx.doi.org/10.1007/s12289-021-01642-8.
[15] Krogh C. KinDrapeMAX. 2023, http://dx.doi.org/10.5281/ZENODO.7525530.
[16] Mack C, Taylor HM. The fitting of woven cloth to surfaces. J Text Inst Trans 1956;47(9):T477–88. http://dx.doi.org/10.1080/19447027.1956.10750433.
[17] Van Der Weeën F. Algorithms for draping fabrics on doubly-curved surfaces. Internat J Numer Methods Engrg 1991;31(7):1415–26. http://dx.doi.org/10.1002/nme.1620310712.
[18] Krogh C, Bak BL, Lindgaard E, Olesen AM, Hermansen SM, Broberg PH, et al. A simple MATLAB draping code for fiber-reinforced composites with application to optimization of manufacturing process parameters. Struct Multidiscip Optim 2021;64:457–471. http://dx.doi.org/10.1007/s00158-021-02925-z.
[19] Krogh C, Bak BL, Lindgaard E, Olesen AM, Hermansen SM, Broberg PH, et al. KinDrape. 2020, http://dx.doi.org/10.5281/ZENODO.4316861.
[20] Mitchell JS, Mount DM, Papadimitriou CH. The discrete geodesic problem. SIAM J Comput 1987;16(4):647–68. http://dx.doi.org/10.1137/0216045.
[21] The MathWorks, Inc. Global optimization toolbox. 2022, URL https://se.mathworks.com/products/global-optimization.html.
[22] Sørensen SN, Sørensen R, Lund E. DMTO - a method for discrete material and thickness optimization of laminated composite structures. Struct Multidiscip Optim 2014;50(1):25–47. http://dx.doi.org/10.1007/s00158-014-1047-5.
[23] Lozano GG, Tiwari A, Turner C, Astwood S. A review on design for manufacture of variable stiffness composite laminates. Proc Inst Mech Eng B 2016;230(6):981–92. http://dx.doi.org/10.1177/0954405415600012.
[24] Potter K, Khan B, Wisnom M, Bell T, Stevens J. Variability, fibre waviness and misalignment in the determination of the properties of composite materials and structures. Composites A 2008;39(9):1343–54. http://dx.doi.org/10.1016/j.compositesa.2008.04.016.